THE PECULIAR LIGHT CURVE OF THE SYMBIOTIC STAR AX PER OF THE LAST 125 YEARS

Elia M. Leibowitz and Liliana Formiggini
Wise Observatory and School of Physics and Astronomy, Raymond and Beverly Sackler Faculty of Exact Sciences,
Tel Aviv University, Tel Aviv 69978, Israel; elia@wise.tau.ac.il

ABSTRACT

We analyze the optical light curve (LC) of the last 125 years of the symbiotic star AX Per through some remarkable correlations that we discovered in its power spectrum (PS). The data were assembled from the literature and from the American Association of Variable Stars Observers database. A series of six major outbursts dominate the LC. They are presented in the PS as 13 harmonics of the fundamental frequency $f_a = 1/P_a = 1/23{,}172$ day^{-1}. We refer to them as the "red" frequencies. Oscillations with the binary periodicity of the system $P_b = 1/f_b = 681.48$ days are also seen in the LC, with particularly large amplitudes during outbursts. The f_b peak in the PS is accompanied by 13 other peaks on each side, which we refer to as the "blue" frequencies. A distinct structure in the frequency distribution of the blue peaks, as well as in their peak power, is best interpreted as reflecting beating of the 13 "red" frequencies with the binary one. We suggest, following others, that the major outbursts of the system result from events of intense mass loss from the giant star. Mass accretion onto the hot component, partially through the L1 point of the system, took place in the last 125 years at a rate that oscillated with the 13 first harmonics of the f_a frequency. The binary orbit is slightly eccentric and periastron passages induced modulation of the L1 accretion at the binary frequency. Hence the f_b oscillations in the brightness of the star of an amplitude that is modulated by the "red" frequencies of the system.

Key words: binaries: symbiotic – stars: individual (AX Per)

Online-only material: supplemental data (MRT)

1. INTRODUCTION

AX Per is one of the well studied prototypes of the symbiotic stars. The stellar system consists of a giant of type M4.5 III (Murset & Schmid 1999) and a hot component, most likely a white dwarf, that are in a binary orbit around each other with a period of some 682 days. This has been established photometrically as well as in radial velocity measurements (Mikolajewska & Kenyon 1992; Fekel et al. 2000). A thick wind is emanating from the red giant. The gaseous medium is heated by the UV radiation of the hot component, producing the bright emission lines that characterize the spectrum of the object (Iijima 1988; Mikolajewska & Kenyon 1992; Ivison et al. 1993, Skopal et al. 2001).

The light curve (LC) of the star is characterized by brightness variations of amplitude 0.1–0.4 mag alternating with epochs of activity characterized by variations reaching amplitudes of up to 3 mag. The binary period of the system has long been recognized as a major modulating agent of the optical output. The light oscillations are mostly attributed to the well known reflection effect in binary systems by the giant star (Formiggini & Leibowitz 1990). Skopal (1994) has shown that in the geometry of the system, heating and ionization of the thick wind emanating from the giant due to collision with the wind of the hot component and to its UV radiation are even more efficient in introducing variations with the binary cycle. In a few cycles of the binary period, eclipses of the hot component have also been identified (Skopal 1994; Skopal et al. 2001, 2011). These interpretations may be adequate for explaining the oscillations during quiescence states but not the wild fluctuations during the outbursts of the system. Also, the energy source, as well as the physical process or processes that give rise to these outbursts, are far from being understood.

More details about the present status of our knowledge about the system, observational as well as theoretical, can be found in a number of excellent investigations in this system performed in the last 25 years (e.g., Mikolajewska & Kenyon 1992; Ivison et al. 1993; Skopal 1994; Skopal et al. 2001, 2011).

AX Per is one of the few stars whose brightness already started being monitored systematically in the 19th century. We are therefore fortunate to be able to construct a LC of the system that extends over the last 125 years. This work utilizes this rich treasure of data, so far not well exploited, in order to extract new knowledge about this system. This paper is the seventh in our long-term study of symbiotic stars using their historical LCs (Formiggini & Leibowitz 1994, 2006, 2012; Leibowitz & Formiggini 2006, 2008, 2011).

2. DATA

AX Per's photometric behavior was first discussed by Lindsay (1932), who, analyzing Harvard plates, noticed variations with period $P \sim 650$ days. The Harvard plates' photographic magnitudes, digitized from the figure of Lindsay, are our first set of data. The total time covered is from 1887 November to 1932 June, corresponding to JD 2,410,590 – 2,426,900. The data up to JD 2,423,600 represent single observations, after this date they are 25 day means. From now on we omit the first two digits, 24, from the JD dates and designate them as "jd."

Another set of photographic data from the Harvard plates, based on a redetermination of the comparison star magnitudes, covers the time interval from jd 23,000 to 31,460 (Payne-Gaposchkin 1946). These are also presented as a plot, from which we extracted a second data set.

Further photographic observations (Wenzel 1956) were retrieved from Figure 4 of Skopal et al. (2000). This set is
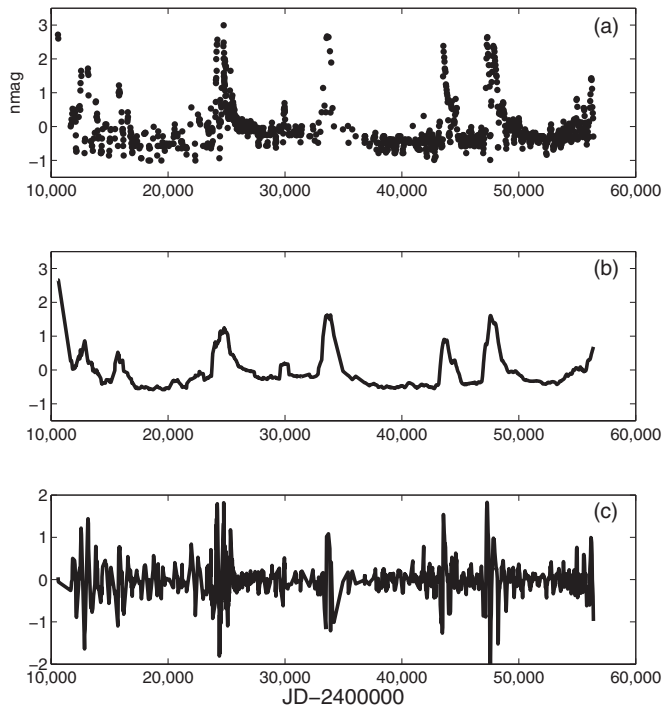
Figure 1. (a) Light curve (LC) of AX Per of the last 125 years. Magnitudes are in normalized units explained in the text. (b) The running mean of the LC with a running window width of 682 day. (c) The difference between the observed LC and the running mean one.
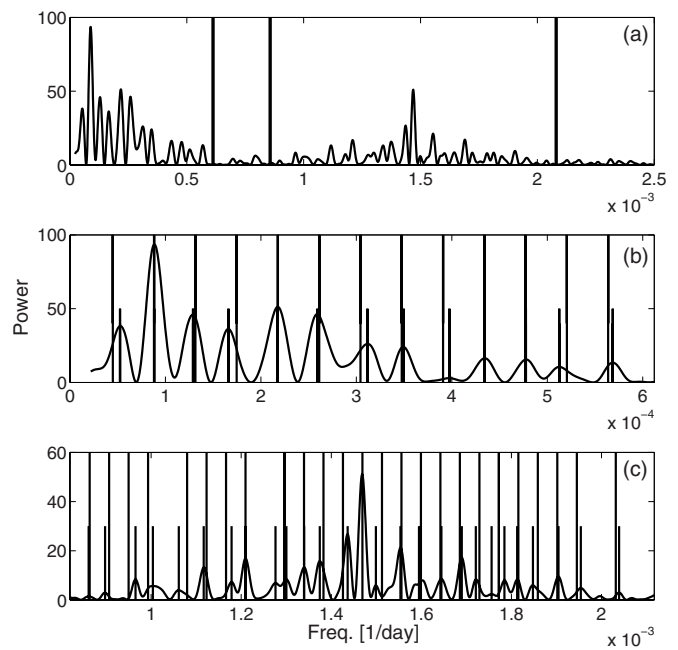
(Supplemental data for this figure are available in the online journal.)

Figure 2. Power spectrum of the LC shown in Figure 1(a). The meaning of the vertical lines is explained in the text.

overlapped by a set of photographic estimates by the Association Francaise des Observateurs d'Etoiles Variables (AFOEV) from jd 32,085 to 40,290.

Regular visual monitoring of AX Per's brightness by the AFOEV and by the American Association of Variable Stars Observers (AAVSO) started around the year 1968. The data gathered by the AFOEV are consistent with those of the AAVSO, and in our analysis we used the AAVSO data updated to 2013 May 5 = jd 56,417, binned into 30 day bins. We note that a few AFOEV data between jd 41,272.5 and jd 41,317.2 show a brightening of the star by more than one magnitude. Following an inquiry with the AFOEV, we discarded these points in the AFOEV LC as spurious (E. Schweitzer 2013, private communication). Jurdana-Sepic & Munari (2010) have published six *B* magnitude values and one *V* magnitude value extracted from historical plates of the Asiago Observatory between the years 1976 and 1985. Finally, we should note that the Mjalkovskij (1977) data were not used owing to the scale discrepancy shown in both the visual and the photographic estimates.

2.1. Scaling the Data

The photographic data, culled from different papers and databases, were checked for scale consistency. In fact, the new estimation of the comparison stars (Payne-Gaposchkin 1946) results in a difference of magnitudes between the two data sets that were retrieved from the Harvard plates. Analyzing the data after jd ∼ 26,000, when the system was in quiescence, we empirically estimated that Lindsay's (1932) magnitudes are 0.24 mag fainter than those of Payne-Gaposchkin (1946). Lindsay's data were shifted and merged with Payne-Gaposchkin's data. As previously noted, the Wenzel (1956) data agree with the AFOEV photographic data and the merging does not required any scale

correction. The final data set of photographic estimates covers the time from jd = 10,590 to 40,290.

The photographic set of data ends during a quiescent state of AX Per when few AAVSO data points are available. Using these short overlapping portions of the LC, we empirically shifted the AAVSO data in order to connect the photographic and the visual data. Figure 1(a) presents the full LC of AX Per so obtained, covering the last 125 years of the star's history. The *y*-axis displays the magnitudes in normal units: $nmag(t) = mean(m) - m(t)$, where $m(t)$ are photographic magnitudes. The displayed LC is essentially the one presented in Skopal et al. (2001, 2011), except for the omission of the spurious AFOEV points mentioned above and the extension of the LC up to 2013 May. Figure 1(b) presents the outcome of an application of the running mean operator on the LC with a running window width of 682 days. We shall refer to this curve in Section 3.6. Panel (c) is the difference between the observed LC and the running mean curve. It shows in particular the strong correlation between the overall brightness of the system and the amplitude of its variation with the binary orbital frequency (see next section).

3. TIME-SERIES ANALYSIS

3.1. Power Spectrum

Figure 2(a) presents the power spectrum (PS) of the LC seen in Figure 1(a). Two clusters of peaks characterize the periodogram. One group is at the low frequency ("red") end, corresponding to periods of the order of 1700 days and longer. The second cluster ("blue") is centered around a distinct peak near the frequency $f_b = 1.47 \times 10^{-3}$ day^{-1}, corresponding to the well known binary period of the system. Here we adopt for this periodicity the value $P_b = 681.48$ days, a choice that will be explained in Section 3.5.

The left heavy vertical line marks the high frequency edge of a frequency band that contains the 13 high "red" peaks in the PS. Figure 2(b) is zoomed in on this passband in which the peak frequencies are marked by the short vertical lines. The two other heavy vertical lines in panel (a) mark respectively the low

and high frequency edges of two passbands on the left and right of the binary frequency f_b, of width equal to that of the "red" band. Panel (c) is zoomed in on the frequency between these two vertical lines. The short low vertical lines mark the frequency f_b and the peak frequencies of the highest 13 peaks in each of the two bands on the left and right of it. We refer to them as the b1 and the b2 peak sequences.

3.2. The "Red" Cluster of Peaks

Even visual examination of Figure 2 reveals that to a very good approximation, the 13 "red" peaks are distributed along the frequency axis with a constant interval between any two neighbors. By the least squares procedure, with the peak power values as weights, we found the set of frequencies such that any two of them are separated by an integral number of a constant value that best fit these 13 "red" peak frequencies. The constant value, termed "quantum" by Broadbent (1955), is found to be $f_a = 4.329 \times 10^{-5}$ day^{-1}, corresponding to the period $P_a = 23{,}100$ days. The long vertical lines in the "red" band in Figure 2(b) mark the frequencies $k/23{,}100$ day^{-1} for all integers $1 \leqslant k \leqslant 13$. We adopt the value $P_a = 23{,}172$ days for reasons explained in Section 3.5.

In view of the above we shall refer to the 13 "red" peaks in the PS as harmonics of the fundamental frequency f_a. We note, however, that this does not necessarily imply that $1/f_a$ is a genuine periodicity of the AX Per system, since the observations cover no more than twice the length of this time interval.

3.3. The "Blue" Cluster of Peaks

We applied the same least-squares procedure to find the "quantum," an integral number that separates any two of the set of 27 peak frequencies in the "blue" PS of the star, marked by the vertical short lines in Figure 2(c). The "quantum" is again found to be f_a, exactly the same as in the "red" sequence. The long vertical lines in panel (c) mark the frequencies of the best-fit set of frequencies with this "quantum" number.

We perform a bootstrap-type test of the null hypothesis that the 13 peaks on each side of f_b are distributed randomly along the "blue" section of the frequency axis of the PS. We consider the standard deviation S of the differences between the observed peak frequencies (short vertical lines in Figure 2) and the predicted frequencies (long lines) as a measure of the quality of the least squares fitting. Within each the two "blue" passbands around f_b we created 16,000 random distributions of 13 frequency values with the constraint that no two numbers among them will be closer to each other than the theoretical resolution of the PS set by the total length of the LC. Applying the least squares procedure on each of these distributions of 27 numbers, we found only 249 cases with an S value as small as or smaller than the one associated with the 27 peaks in the PS of the observed LC. The probability that the 26 observed "blue" peaks around f_b are due to random noise in the LC can therefore be rejected at a 98.4% statistically significant level. The equality of the "quantum" values in the "red" and "blue" sections of the PS reduces the probability of randomness in the distribution of the "blue" peaks to practically zero.

3.4. Correlation in Power

We now consider the values of the maximum power of the 26 peaks of the b1 and the b2 sequences defined above. We combine the powers of the peaks nearest to f_b in the two sequences, then the powers of the second nearest peaks in b1 and
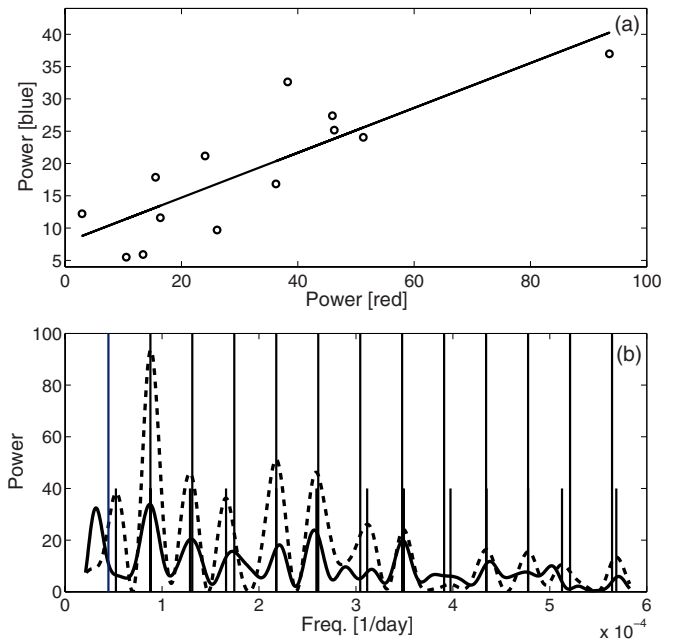
Figure 3. (a) Regression of the power of 13 pairs of peaks, one from the b1 and one from the b2 "blue" sequence peaks in the PS of AX Per, on the powers of the 13 "red" peaks in the PS. (b) The dashed line is the "red" section of the PS of AX Per and the solid line is the sum of the two "blue" sections on the two sides of the binary frequency in the PS, moved to the origin of the frequency axis. The b1 section is considered in reverse direction. See the text for further explanation.

b2, etc. We thus obtain 13 values of power of the 13 pairs of peaks around f_b. Figure 3(a) is a plot of these 13 power values versus the powers of the 13 "red" peaks seen in Figure 2. The line in the figure is the regression line between these two sets of 13 power values. A bootstrap test on a sample of 10,000 sets indicates that the null hypothesis that the two sets are uncorrelated can be rejected at a 99.96% probability. The slope of the line is 0.347 ± 0.168, where the quoted uncertainty indicates the 99% confidence interval around the slope value. Somewhat lower but still statistically significant correlations are also found between the 13 powers of the "red" sequence and the powers of the b1 and the b2 sequences considered separately.

Figure 3(b) demonstrates qualitatively the correlation that we find between the "red" and the "blue" sections of the PS. In it, we plot again as a dashed line the PS in the "red" passband. Superposed on it, as a solid line, is a plot of the sum of the b1 and b2 sections, with f_b set to zero, and where b1 is considered in reverse order, namely from right to left. As in Figure 2, the short vertical lines mark the peak frequencies of the 13 "red" peaks and the long ones mark the frequencies that best fit the "red" peaks with the f_a quantum.

We emphasize at this point that these highly improbable features of the PS are uncovered in the periodogram of the raw LC of the star. In the process of their discovery we have made no assumption concerning the presence of any periodical content in the LC. Even the fact that P_b is the well known binary period of the system has not been used in this analysis.

3.5. Beats

The most natural and straightforward interpretation of the peculiar characteristics of the PS presented in the previous two sections is that they reflect beating of the 13 frequencies of the "red" sequence with f_b, the binary frequency of the system.

Table 1
Parameters of the Function $Y(t)$ That Best Fits the Observed LC

Parameter	P_a (day)	P_b (day)	A_{free} (mag)	θ_{mod}	θ_{free}
Value	23,172	681.48	0.306	0.819	0.860
±uncertainty	125	0.43	0.072	0.035	0.043

Note. The parameters are the frequencies of the two dominant periods in the data, the amplitude of the free f_b oscillator, and the phase constants of the modulated and the free oscillators, relative to jd 51,135.

An LC of oscillations at a frequency f_b and at the 13 first harmonics of frequency f_a that are also beating with frequency f_b, can be expressed mathematically as follows:

$$Y(t) = \sum_{j=1}^{13} A_j \sin[2\pi(jf_a t + \varphi_j)]$$
$$+ \sum_{k=1}^{13} B_k \sin[2\pi(kf_a t + \mu_k)] \sin[2\pi(f_b t + \theta_{\text{mod}})]$$
$$+ C \sin[2\pi(f_b t + \theta_{\text{free}})]. \tag{1}$$

The first sum on the right hand side of the above formula represents free oscillations at the 13 first harmonics of frequency f_a. The second sum represents the beats of these harmonics with frequency f_b. We may also view this sum as representing an oscillator of frequency f_b, modulated by the 13 harmonics of f_a. The last term in the formula is required in order to produce in the PS the prominent peak of the f_b frequency itself. This free f_b oscillator is not necessarily in phase with the modulated one.

By least squares fitting the $Y(t)$ function to the observed LC, we find the values of the two frequencies f_a and f_b, the amplitude of the free oscillator, and the phases of the two f_b oscillators. The least squares procedure also yields the values of the amplitudes and phases of the 13 "red" harmonics, as well as those of the 13 harmonics of the same frequencies that modulate the modulated oscillator. Table 1 lists the values of f_a, f_b, the amplitude A_{free} of the free oscillator, and the phases θ_{mod} and θ_{free} of the modulated and the free oscillators. Here, phase zero is at jd 51,135, the time of maximum radial velocity of the giant as reported by Fekel et al. (2000).

The uncertainty values are estimated on the basis of bootstrap calculations. We consider the residuals of the observed minus theoretical Y value on each time point of the observations as a bank of "errors." We then create a pseudo-observed LC by considering the $Y(t)$ values on each time point, to which we add one number chosen randomly from the error bank. We apply our least squares procedure on this pseudo-observed LC and obtain pseudo-observed values of the five parameters of Table 1. We perform these calculations on a sample of 200 such pseudo-observed LCs. The dispersion of the 200 values so obtained for each parameter defines the corresponding uncertainty number presented in Table 1.

The quality of the fit of the $Y(t)$ function to the observed LC can be appreciated qualitatively by comparing the observed LC, displayed again as the upper curve in Figure 4, to the lower curve, which is the best-fit Y function. The PS of the lower curve is almost indistinguishable from the PS shown in Figure 2.

In the least squares procedure, all the A and B parameters are treated as entirely independent, free parameters. We find that the resulting B_k amplitudes are linearly correlated with the
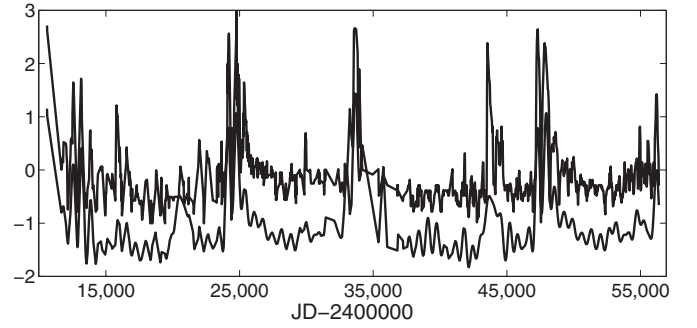
Figure 4. Upper curve: observed LC of AX Per. Lower curve: the $Y(t)$ function, i.e., the analytical beats model, best fitted to the observed data.

resulting A_j amplitudes, as expected if the LC of the star does indeed represent physically beating frequencies.

We point out that our presentation of the theoretical LC in Figure 4 and the demonstration of its good fit to the observation are not intended to be regarded as evidence for the validity of our beating model. The figure serves only to show that the LC of the star may well be simulated by a beating model with an appropriate choice of parameters. The evidence for the beats lies entirely in the peculiar features and correlations that we discover in the PS of the raw data that are clearly nonrandom at a highly statistical significance level.

3.6. Comments on the Fitted Curves

1. The decomposition of the long-term, outburst-structured variations of the LC into the 13 harmonic oscillations is of course implied by the PS but it is not an important part of the peculiarities of the PS, nor is it essential in our discussion of them. We obtain practically the same theoretical LC and PS when considering a three-component function consisting of the running mean LC shown in Figure 1(b), a free oscillator with the f_b frequency, and a second oscillator of the same frequency modulated by the running mean, multiplied by a constant number. This is of course not an independent result but rather a consequence of the faithful representation of the running mean function by the 13 harmonics of f_a. In the least-squares fitting of this function to the data there are only five free adjustable parameters, namely, the frequency f_b, the phases of the free and modulated f_b oscillators, the amplitude of the free oscillator, and the constant of proportionality mentioned above. The resulting f_b value and the phases of the free and modulated oscillators are practically identical to the numbers presented in Table 1. The amplitude of the free oscillator is also consistent, within the uncertainty interval, with the value given in Table 1. The constant of proportionality also takes a similar value to the slope of the regression line presented in Section 3.4.

2. The upper curve in Figure 5 is an extension of the PS of the observed LC beyond the frequency limit 1/450 day^{-1} of the PS seen in Figure 2, to the limit 1/200 day^{-1}. This is roughly three times the mean Nyquist frequency of the LC time series. The lower curve is the same for the theoretical function $Y(t)$. The theoretical function is of course entirely noiseless. It represents only the time variation that we set, namely, just the f_a frequency with its 13 harmonics, the f_b frequency, and the corresponding beat frequencies. The features in the lower PS must therefore represent interferences among these frequencies due to the final length of the LC and to the nonequal sampling of
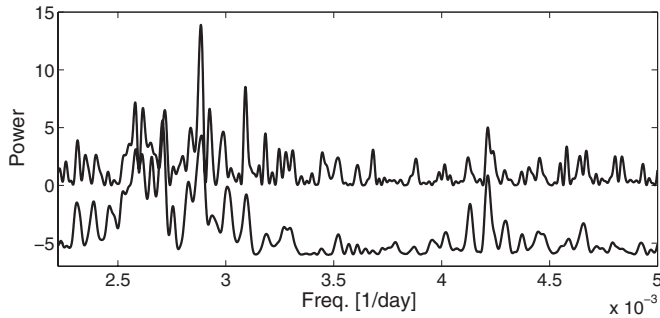
Figure 5. Upper curve: PS of the observed LC in the period range 450–200 days. Lower curve: the same for the best-fit theoretical $Y(t)$ function.

it. This suggests that the nearly identical spectral features in the PS of the real data seen in the upper curve reflect similar interferences among the same basic frequencies, implying that these frequencies are indeed underlying the observed LC.

3. Skopal et al. (2012) performed precise photoelectric photometry of AX Per during some parts of the time interval jd 53,000 < t < jd 56,000. They report on large oscillations of the system at quiescence phases as well as during outbursts that are significantly out of phase of the P_b periodicity that is almost always prevalent in the LC. These out-of-phase oscillations are also apparent in the AAVSO data. The f_b variability becoming out of phase during this time interval is well described by the theoretical $Y(t)$, although not with the details of the structure that the LC assumed at that time. It is even predicted by the function $Y(t)$ when fitted to the observed LC from which the data points of the above time interval are omitted. It seems that the out-of-phase variations at that time result from interference of frequencies involved with the $Y(t)$ function.

3.7. Macro versus Micro Presentation

Our present work is an attempt to understand the gross features of the optical photometric LC of AX Per. It addresses the time variations in the brightness of the star of the order of 0.5 mag and larger in brightness, and of a timescale of 450 days and longer. The system is varying also on shorter timescales and with smaller amplitudes in brightness. The out-of-phase oscillations mentioned in the previous section are one example. Also, Skopal et al. (2012), as well as the LC of the star presented in this work, show that the P_b periodicity is hardly being preserved on the "micro" scale. This is apparent in the varying shape of the P_b cycle even at quiescence states of the star. It is also manifested by the fact that the time interval between apparent neighboring minima is varying by up to 100 days or more around the P_b periodicity. For example, the time intervals between the apparent minima of seven consecutive P_b cycles between jd 46,500 and 51,500 are 602, 678, 678, 693, 723, and 662 days. These different values are independent of the binning operation that is applied on the LC. We obtain nearly the same numbers when we consider the AAVSO LC binned into 10 or 30 day bins. Minima measured photoelectrically show similar excursions away from their expected times of occurrence. It should be noted, however, that some variation from a strict binary cycle may be attributed to variations in the ionization structure of the giant wind (Skopal 1998). In Figure 1(c) one can also identify variability on shorter timescales and smaller amplitudes than the variations on the binary cycle

periodicity. The 681.5 day periodicity is, however, a robust feature of the system. The centers of the "micro" variability excursions preserve their periodicity and phasing throughout the last 125 years of the star's history.

In this work we are concerned only with the "macro" variability of the system. An underlying assumption in our approach is that the gross features of the LC carry information about the clocks that control the timing of the major events in the dynamics of the system. We assume that the effects of these clocks may indeed be decoupled from the micro-variations without losing this information.

All variations that we refer to as "micro" have to do with the physical processes that transform the gravitational energy released in the accretion process, and possibly also in the nuclear reaction on the surface of the white dwarf, to the optical output of the system. These are taking place in various components of the system such as the winds of the two stars, an inter-binary and circumbinary nebulosity, gaseous streams, and possibly also an accretion disk. They depend naturally on the dynamics and kinematics of these components, as well as on details of the thermodynamical processes within them. In view of their relatively small effects on the LC, these processes may be regarded as perturbations on the more orderly temporal behavior of the basic energy generation processes in the system. The detailed study of these perturbations is beyond the scope of this paper.

3.8. The Relation with the Spectroscopic Ephemeris

If one assumes that the orbit of the AX Per binary system is circular, then the maximum radial velocity of the giant occurs a quarter of a cycle after the time of inferior conjunction of that star. In Table 1 we reported that the phases of minimum light of the modulated and the free oscillators precede the phase of maximum radial velocity as given by Fekel et al. (2000) by less than 0.25. Note, however, that for $P_b = 681.48$ days, the two very deep minimum points measured during two major outbursts, at jd 24,389 and jd 47,555 (see Figure 1(a)), are indeed at phase 0.75.

4. DISCUSSION

In this section we propose a qualitative physical model for the AX Per symbiotic system that is likely to be a realization of the mathematical beating model suggested by the observations.

4.1. The Source of the Continuum Radiation

The main sources contributing to the optical continuum of AX Per are represented by the hot component, the giant, and the nebula (Skopal 2005). The hot component of the system and its close environment are undergoing partial and sometimes total eclipses by the giant of the system, giving rise to the modulations at the binary period of the system. These variations are also augmented by the reflection effect from the surface of the giant and from its thick wind (see Section 1). However, the periodic variations in the aspect ratio of the revolving AX binary system can hardly explain some basic observed features of the LC of the star.

As noted in Section 3.7, the observed times of minimum light of individual cycles have frequent variations that may reach a distance of more than 100 days away from the nominal times of a strictly P_b periodicity. In phase space these differences are sometimes as large as 0.15. It is hard to see how minima that are due to eclipses and to the reflection effect, being

mostly geometrical in origin, can differ that much from the strictly periodic times of inferior conjunction. Furthermore, the amplitude of light variations due to an eclipse of the light source or to varying aspects of a medium reflecting its light are to first approximation a given fraction of the source light intensity. The measured amplitude in magnitude units of variations due to these mechanisms alone should be roughly independent of the light intensity of the source. This is clearly not the case in AX Per, where the amplitude in magnitude units of the P_b variations during outbursts may be 3 or more times the mean amplitude during quiescence (see Figure 1(c)). The amplitude at quiescence intervals is also varying considerably with time.

The system must therefore also include an additional light source that is fluctuating at the binary frequency, nearly in phase with the eclipse and the reflection effects. The amplitude of this fluctuating source is strongly modulated by the same 13 "red" frequencies that gave the LC of the star the outbursts structure that it had in the last 125 years (Figure 1(b)).

4.2 Outbursts

The major energy source of the radiation of AX Per is in an accretion of material from the wind and possibly also from the atmosphere of the giant star onto the hot component of the system. This process releases large quantities of gravitational energy. It may also supply fuel to an ongoing nuclear burning process on the surface of the white dwarf. This has been proposed already more than 20 years ago by Mikolajewska & Kenyon (1992) and Ivison et al. (1993). The outburst episodes would then be events where extra material is ejected from the atmosphere of the giant star (Skopal et al. 2011). The rate of mass loss from the giant is most likely controlled by an intrinsic parameter or parameters of this star. Skopal et al. suggested, for example, that during one active phase of the system that they have studied, the radius of the giant increased by more than 10% (from 102 R_o to 115 R_o). Variations in the mass loss rate may also be associated with variations in a global magnetic field in the outer layers of the star.

To date, there is no direct observational indication of a global magnetic field on the surface of the giant of AX Per. However, nondetection is by no means a confirmation of the absence (see, for example, the detection of the magnetic field in Arcturus, the presence of which was unrecognized until very recently; Sennhauser & Berdyugina 2011). Cyclic or quasi-cyclic variability in the intensity, perhaps also in polarity, of stellar magnetic fields is ubiquitous, not only in our sun, but also in a wide range of different stars, including red giants (see, for example, Dal et al. 2012, and many references therein). Also, in a recent paper Olah et al. (2013) reported on photometric observations in 3 K giant stars that vary on timescales of years, possibly with periods of 5 or 10 yr. These authors suggest that the photometric variability is a testimony on surface magnetic field variations of the same timescale.

We note in connection that in the series of papers of the present authors listed in Section 1, we have pointed out the possibility of and produced at least circumstantial evidence for the presence of magnetic fields in the atmosphere of the cool components of a few well known symbiotic systems.

The outburst structure of the LC is accordingly most likely an optical manifestation of variations in the value of the relevant intrinsic parameter of the giant star, which we assume for the rest of our discussion to be the radius of the star. The PS then shows that during the last 125 years the giant was pulsating as a harmonic oscillator of the 13 frequencies of the "red" peaks

of the PS. According to Skopal et al. (2001), if the inclination angle of the orbital plane is $i = 90°$ the radius of a tidal lobe filling giant is 102 R_o, while if $i = 70°$ the radius is 170 R_o. In fact, Mikolajewska & Kenyon (1992) have also suggested that the orbital inclination might be approximately 70° with the red giant filling its tidal lobe. It would therefore seem that at each mode of the giant pulsations, accretion of matter through the L1 point of the system may have taken place. Alternatively or in addition, each mode of this pulsation created a corresponding mode of oscillations in the intensity of the wind emanating from the giant and consequently also in the rate of wind accretion of matter onto the hot component and through the L1 point. The combined effect of the 13 frequencies' oscillations in the accretion rate gave rise to the observed series of outbursts of the system.

4.3. The Modulated Oscillator

Accretion through the L1 point of the system is thus modulated with the frequency of any one of the star pulsation modes. If the binary orbit is non circular, the excess mass flow through the L1 point will also be modulated at the binary frequency. This will be translated to variations in the luminosity of the system at this frequency, with maximum light reached around a certain specific phase after periastron (Lajoie & Sills 2011). Details of the process of the release of energy, gravitational and/or nuclear, associated with varying accretion rate onto the hot component have been discussed by Sokoloski et al. (2006) in the context of another well studied symbiotic star, Z And. This mechanism may be suggested as the source of the very large amplitudes of the binary oscillations during outbursts.

We may describe the process in a slightly different language. Due to a slight eccentricity of the binary orbit, the mass accretion through the L1 point of the system is modulated at the binary frequency. The mass flowing toward the L1 point is supplied by the giant wind. Therefore, the amplitude of f_b oscillations in the accretion rate is modulated by the 13 frequencies of the giant pulsations. This is the physical origin of the second sum on the right hand side of Equation (1).

Fekel et al. (2000) analyzed all the radial velocity data for the giant star of AX Per that were available at the time of their work. They concluded that the binary orbit of this system is circular, following the precepts outlined by Lucy & Sweeney (1971). These authors have found, however, an orbital solution with a nonzero eccentricity.

We have reanalyzed the radial velocity curve of AX Per as given in Table 8 in Fekel et al. (2000). Using formula (1) in Lucy & Sweeney (1971), we find a best-fit orbital solution with eccentricity $e = 0.052$. However, as noted by Fekel et al., we also find that due to the noise in the data, a circular solution is quite consistent with the data. In other words, the null hypothesis that the orbit is circular cannot be rejected by the currently available data. But as stated by Feigelson & Babu (2013), "... the null hypothesis can be rejected at a given level of significance, but the null hypothesis can not formally be accepted." Also, in a recent paper Lucy (2013) presented a new Bayesian inference for orbital eccentricities of single line spectroscopic binaries. One of his conclusions is that "Systems assigned $e = 0$ (according to these earlier tests) should preferably have upper limits e_U computed." In Table A.3 in Lucy's paper it is also shown that upper limits for eccentricities could be significantly larger than the values derived by the least squares procedure. Thus a slightly noncircular orbit of the AX Per binary system is certainly not ruled out by the currently available observations. Lajoie & Sills

([2011](#)) have shown theoretically that at least for some binary systems, an eccentricity of the order of 0.1 is enough to modulate an accretion process at the binary frequency.

4.4. The Two Oscillators

According to our proposition, two distinct oscillations are responsible for the variations of the brightness of AX Per at the binary period, the varying aspect ratio due to the system binary revolution, and the varying mass flow through L1 due to the system eccentricity. This fact has been so far elusive because the resulting two f_b oscillations in the light of the system have nearly the same phase. The slight difference between these two phases, as presented in Table [1](#), could be real but analysis shows that it is statistically not significant.

The coincidence of near equality of the phases of the two oscillators may be regarded as a weakness of our model, but one has to bear in mind that such close phases occur with a probability that is no smaller than any other specific phase difference between the two. What enabled us to disentangle the effects of the two distinct oscillators in spite of their nearly equal phases is our analysis of the 125 year LC of the star in its entirety and not of only a limited section of it as was done so far by most studies of the system variability.

4.5. The Free Oscillator

The free oscillator term, the last one on the right hand side of Equation ([1](#)), represents the variability that is due to eclipses and the reflection effect. The amount of hot component light that is blocked by the giant and the amount reflected from the giant surface or from any other fixed material element in the rotating binary system are at any given phase determined primarily by the geometrical size of the giant star and perhaps also of the optically thick wind around it. To first approximation, these geometrical parameters are independent of the luminosity of the system. This is why this P_b variability is represented by an unmodulated, free oscillator.

The phase of minimum light of the unmodulated oscillator that is due to eclipses should be the mark of inferior conjunction of the giant. Unfortunately, it cannot be determined by photometric measurements due to the effect of reflection that does not necessarily attain its maximum brightness level at superior conjunction of the giant. Also, in general, the eclipse effect is being masked by interference with the oscillations of the modulated oscillator. The latter is dominating the LC because of its larger amplitudes. The cycle of this oscillator is much less well defined on the "micro" level. This is due to the nature of the chain of physical processes that transform the variations in the gravitational/nuclear releases of energy to optical light fluctuations. Note, however, that when circumstances in the system allow the identification of an eclipse, as was probably the case at the two dates mentioned in Section [3.8](#), the eclipse had indeed preceded the phase of maximum radial velocity of the giant by quarter of a cycle.

5. SUMMARY AND CONCLUSION

We discover a certain structure in the PS of the LC of the symbiotic star AX Per as well as a tight linear relation between the powers of its apparent peaks. These features are nonrandom at a very high statistically significant confidence level. The

outbursts of the system that characterize the long-term structure of the LC can be decomposed into 13 interfering harmonic oscillations of periods of thousands of days. We suggest that these 13 "red" frequencies are those of oscillations in the value of a fundamental parameter of the giant atmosphere, most likely the radius of the star. These oscillations drive oscillations at the same frequencies in the rate of mass loss from the giant and therefore also of the accretion rate onto the hot component. This is the origin of the series of the outbursts of the star. Some of the accretion onto the hot component is by overflow of material through the L1 point of the system. Due to a slight eccentricity of the binary orbit, this flow of matter is also modulated by the binary frequency. The beat of the 13 "red" frequencies with the binary one gives the "blue" section of the PS of the LC its observed peculiar structure. It also explains the linear relation that is found between the power of the "blue" peaks in the PS and that of the "red" peaks.

If the giant star continues to oscillate with the f_a frequency into the future, one could predict that the outburst that the system is currently undergoing will reach its peak luminosity sometime around jd 56,840 (2014 June/July).

REFERENCES

Broadbent, S. R. 1955, Biometrika, 42, 45
Dal, H. A., Sipahi, E., & Ozdarcan, O. 2012, PASA, 29, 150
Feigelson, E. D., & Babu, G. J. 2013, in Planets, Stars and Stellar System, ed. T. D. Oswalt (Dordrecht: Springer), 445
Fekel, F. C., Hinkle, K. H., Joyce, R. R., & Skrutskie, M. F. 2000, AJ, 120, 3255
Formiggini, L., & Leibowitz, E. M. 1990, A&A, 227, 12
Formiggini, L., & Leibowitz, E. M. 1994, A&A, 292, 534
Formiggini, L., & Leibowitz, E. M. 2006, MNRAS, 372, 1325
Formiggini, L., & Leibowitz, E. M. 2012, MNRAS, 422, 2648
Iijima, T. 1988, Ap&SS, 150, 235
Ivison, R. J., Bode, M. F., Evans, A., Skopal, A., & Meaburn, J. 1993, MNRAS, 264, 875
Jurdana-Sepic, R., & Munari, U. 2010, PASP, 122, 35
Lajoie, C. P., & Sills, A. 2011, ApJL, 726, 67L
Leibowitz, E. M., & Formiggini, L. 2006, MNRAS, 366, 675
Leibowitz, E. M., & Formiggini, L. 2008, MNRAS, 385, 445
Leibowitz, E. M., & Formiggini, L. 2011, MNRAS, 414, 2406
Lindsay, E. M. 1932, BHarO, 888, 22
Lucy, L. B. 2013, A&A, 551, A47
Lucy, L. B., & Sweeney, M. A. 1971, AJ, 76, 544
Mikolajewska, J., & Kenyon, S. J. 1992, AJ, 103, 579
Mjalkovskij, M. I. 1977, PZP, 3, 71
Murset, U., & Schmid, H. M. 1999, A&AS, 137, 473
Olah, K., Moor, A., Strassmeier, K. G., Borkovits, T., & Granzer, T. 2013, AN, 334, 625
Payne-Gaposchkin, C. 1946, ApJ, 104, 362
Sennhauser, C., & Berdyugina, S. V. 2011, A&A, 529, 100
Skopal, A. 1994, A&A, 286, 453
Skopal, A. 1998, A&A, 338, 599
Skopal, A. 2005, A&A, 440, 995
Skopal, A., Pribulla, T., Wolf, M., Shugarov, S. Y., & Jones, A. 2000, CoSka, 30, 29
Skopal, A., Shugarov, S., Vavnko, M., et al. 2012, AN, 333, 242
Skopal, A., Tarasova, T. N., Cariková, Z., et al. 2011, A&A, 536, 27
Skopal, A., Teodorani, M., Errico, L., et al. 2001, A&A, 367, 199
Sokoloski, J. L., Kenyon, S. J., Espey, B. R., et al. 2006, ApJ, 636, 1002
Wenzel, W. 1956, Mitt. Verand. Sterne, 227